THE JOURNAL OF PHYSICAL CHEMISTRY LETTERS
A JOURNAL OF THE AMERICAN CHEMICAL SOCIETY

pubs.acs.org/JPCL Letter

Modeling Electrochemical Vacancy Regeneration in Single-Walled Carbon Nanotubes

Jana Jelušić, Jan Paul Menzel, Quentin C. Bertrand, Robert H. Crabtree, Hailiang Wang, Gary W. Brudvig, and Victor S. Batista*

Cite This: J. Phys. Chem. Lett. 2024, 15, 7788−7792 Read Online

ACCESS | Metrics & More | Article Recommendations | Supporting Information

ABSTRACT: Synthesis-induced defects in single-walled carbon nanotubes (SWCNTs) enable diverse catalytic reactions, but the nature of catalytic intermediates and how active species regeneration occurs are unclear. Using a quantum mechanics/molecular mechanics (QM/MM) hybrid methodology based on density functional theory (DFT) and a classical force-field, we explore the reactivity and electrochemical regeneration of a vacancy defect in a zigzag SWCNT. Our findings indicate that hydrolysis of the defect forms a ketone group on one carbon atom and C−H bonds on two adjacent carbons. Applying an electrochemical potential of E_{SHE} = −0.740 V triggers a proton-coupled electron transfer (PCET), converting the ketone to a hydroxyl group. Further reduction at E_{SHE} = −1.08 V induces another PCET, expelling the hydroxyl as water and forming an active carbon with carbene character that can react with hydrogen peroxide and perchlorate. The hydrogen atoms on neighboring carbons prevent further water dissociation, maintaining the catalytic vacancy.

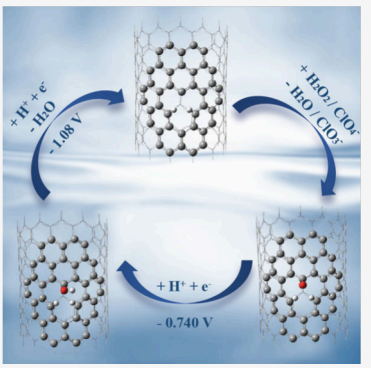

Single-walled carbon nanotubes (SWCNTs) have attracted considerable interest in research and practical applications due to their exceptional properties, such as mechanical strength, electrical and thermal conductivity, and chemical stability.[1,2] These attributes render SWCNTs ideal for many applications, including energy conversion, catalysis, electronics and semiconductors, hydrogen storage, drug delivery, and sensing technologies.[3,4] They serve as cost-effective alternatives to metals in scenarios where they facilitate catalysis,[5] either on their own or when augmented with catalysts deposited on their surface.[6−9] Despite pristine SWCNTs consisting solely of stable sp^2-hybridized carbons, their inherent curvature can introduce a minor sp^3 character.[10] Earlier studies have shown that carbon can exhibit hybrid phases through combinations of hybridized orbitals, such as sp^2 + sp^3.[11] Nonetheless, the presence of carbon atoms lacking sp^2 character results in defects on the nanotube surface.[12] The electrocatalytic activity of SWCNTs has been correlated to the curvature of the nanotube and the presence of imperfections or atomic vacancies on the surface.[13−15] Significant progress has been made to understand how vacancies influence the physical behavior of nanotubes.[16] However, an outstanding challenge is to understand the correlation between catalytic activity and the presence of defects.

Structural defects in SWCNTs are an inherent outcome of the manufacturing process, which typically involves vigorous acid treatments to enhance the hydrophilic nature of SWCNTs and to remove metal contaminants.[17] Numerous studies have been devoted to modeling and characterizing these vacancies, acknowledging that electron mobility tends to increase with their presence.[14,18,19] Furthermore, it is anticipated that single-atom defects significantly influence the physical and chemical properties of carbon-based materials.[20] For instance, it has been shown that not only do defect sites serve as preferred binding locations for single gold (Au) atoms, but they also enhance charge transfer from the Au atom to reactant oxygen (O_2) molecules.[21] The significance of vacancies is widely recognized, with theoretical investigations primarily focusing on the vacancy defect, characterized by the removal of a single carbon atom from the nanotube. These types of vacancies are among the most common and stable defects.[22,23] Despite the acknowledged importance of vacancies, our comprehension of their role in enhancing the reactivity on the surface of SWCNTs remains limited, partly due to the challenges associated with modeling such systems reliably and efficiently.

We now present our findings on the reactivity of a single-carbon vacancy (structure **1** in Figure 1), its hydrolysis, and its subsequent electrochemical regeneration. The vacancy regeneration following the completion of a catalytic cycle requires energy input. While photoexcitation has been suggested as a means to achieve this,[20] to our knowledge, no prior work has reported on modeling of electrochemical regeneration of vacancies.

Received: May 2, 2024
Revised: July 3, 2024
Accepted: July 17, 2024

https://doi.org/10.1021/acs.jpclett.4c01293
J. Phys. Chem. Lett. 2024, 15, 7788−7792

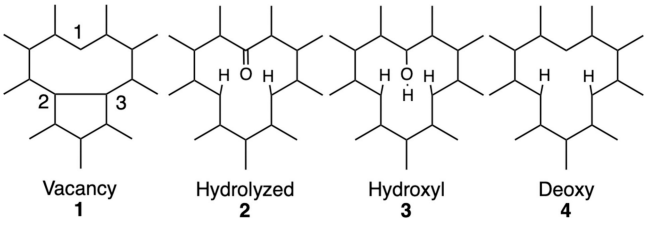

Figure 1. Structural defects of SWCNTs discussed in the text: **1** shows the initial form of the vacancy, including the carbon atom numbering used in the text, **2** is the hydrolyzed form with two C−H bonds and a keto group, **3** is the one-electron, one-proton reduced hydroxyl form, and **4** is the deoxy form that has retained the two C−H bonds.

Among the nine carbon atoms immediately surrounding the vacancy, our findings indicate that the three carbons labeled as C-1, C-2, and C-3 in structure **1** of Figure 1 exhibit the highest reactivity. In aqueous conditions, hydrolysis of the nanotube leads to the formation of a ketone group at the C-1 carbon, while the two carbon atoms, C-2 and C-3, bind hydrogen atoms from water (Figure 2, left, and structure **2** in Figure 1). Subsequently, we explored the reactivity of the newly formed structure as the next step of the mechanism.

In the fully aqueous system, applying an electrochemical potential of E_{SHE} = −0.740 V is sufficient to initiate a proton-coupled-electron transfer (PCET) process, converting the ketonic oxygen into a hydroxyl (Figure 2, right, and structure **3** in Figure 1). A subsequent PCET step, at E_{SHE} = −1.08 V, leads to the release of H_2O, resulting in the formation of the deoxy form **4**. This leaves an open reactive site at C-1 (structure **4** in Figure 3). In the deoxy form, the retention of hydrogen atoms on C-2 and C-3 prevents a water hydrolysis reaction (Figure S4), and C-1 maintains its two-coordinate reactive state, characterized by pronounced carbene character (Figure S2).

This reaction sequence is predicted to facilitate useful reductive chemistry. Beyond water, hydrogen peroxide and perchlorate can also engage with the restored nanotube vacancy (structure **4** in Figures 1 and 3). The detection of H_2O_2, in a potential sensor application, holds particular significance in the biomedical field, as its abnormal production is associated with oxidative damage.[24,25] The reaction involves a proton, an electron, and H_2O_2 interacting with the free carbon atom, resulting in the formation of a ketone or a hydroxyl group on the active carbon, and the release of H_2O (Figure 4). The interaction between H_2O_2 and the two-coordinate carbon of **4** is advantageous, leading to the formation of a ketone or a hydroxyl group on the active carbon, which can depart as H_2O, thereby regenerating the initial state.

Perchlorate (ClO_4^-), a widespread water contaminant known for its thyroid toxicity,[26−28] typically requires harsh conditions or multicomponent enzyme combinations for reduction. Previous studies have suggested the reduction of ClO_4^- to ClO_3^- as the rate-limiting step.[28] When ClO_4^- interacts with the active C-1 carbon in the deoxy vacancy (structure **4** in Figures 1 and 3), it is observed to transition into the hydrolyzed structure (structure **2** in Figures 1 and 3), accompanied by the release of ClO_3^- (Figure 5). The ketone in **2** can then be converted into the hydroxyl group of **3** through the mechanism described earlier. The subsequent application of the same potential (E_{SHE} = −1.08 V) enables the regeneration of the active carbon in the deoxy form, with the release of H_2O.

Hydrogen evolution is a common competitor in electroreduction with metal catalysts but here we found no good pathway for this process. Selectivity for reduction of ClO_4^- or H_2O_2 is of course highly desirable so that energy is not wasted on H_2 production.

In summary, we find that a single vacancy in SWCNTs exhibits high reactivity, facilitating the formation of a ketone, and thus deactivating the vacancy. However, by applying a negative potential of E_{SHE} = −0.740 V, this ketone can undergo reduction and protonation to yield a hydroxyl species, with further reduction and protonation resulting in the release of water and the regeneration of the active sp^2 carbon. This process indicates that vacancies do not have to be permanently hydrolyzed but can be regenerated for multiple reactions under appropriate redox conditions. These findings shed light on how electrocatalytic activity is possible in defective SWCNTs without the need for metal ions or other additives.

COMPUTATIONAL METHODS

The model nanotube was created using a Web-Accessible Nanotube Structure Generator, TubeGen Online − Version 3.4.[29] All geometry optimizations and frequency calculations were carried out at the density functional theory (DFT) level, utilizing the ωB97X-D functional[30] with Grimme's D2 dispersion correction.[31] Employing the ONIOM (Our own N-layered Integrated molecular Orbital and molecular Mechanics) method,[32] the system was divided into two layers treated with different levels of theory. The quantum

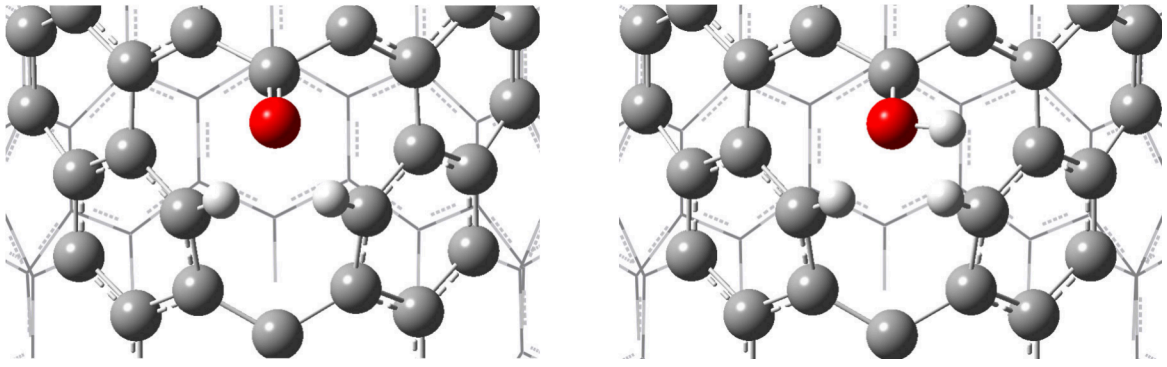

Figure 2. ***Left:*** H_2O binding at the vacancy results in formation of a ketone group and hydrogenation of C-2 and C-3. ***Right:*** The ketone is transformed to a hydroxyl group at an electrochemical potential of E_{SHE} = −0.740 V. Oxygen is colored red, carbons gray, and hydrogens white.

https://doi.org/10.1021/acs.jpclett.4c01293
J. Phys. Chem. Lett. 2024, 15, 7788−7792

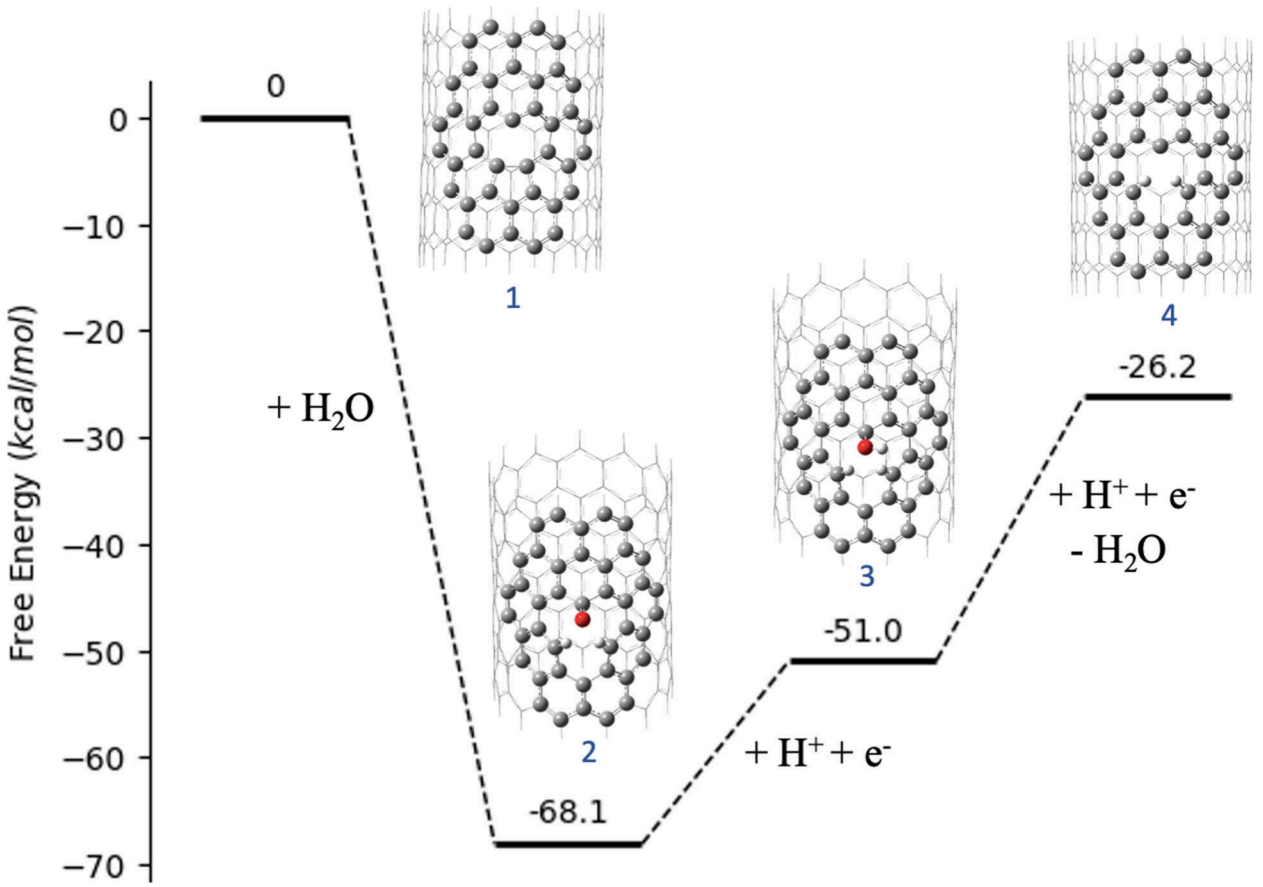

Figure 3. Energetics of the proposed mechanism for vacancy regeneration in SWCNTs. Oxygen is colored red, carbons gray, and hydrogens white.

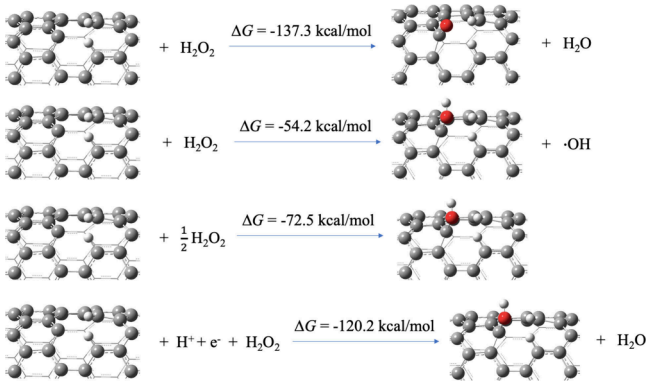

Figure 4. Four distinct pathways for the reaction of H_2O_2 with the active carbon, leading to the formation of a ketone or a hydroxyl group and two C−H bonds. Following the formation of the hydroxyl group, the same potential (E_{SHE} = −1.08 V) is required to regenerate the initial active carbon. Oxygen is colored red, carbons gray, and hydrogens white.

mechanical (QM) layer was addressed at the "high" DFT level, while the molecular mechanical (MM) layer was handled at the "low" level of theory. This approach allows for the treatment of the chemically significant portion (i.e., the vacancy) alone with the accurate yet costly QM method, whereas the remainder of the system is treated using the less accurate but more efficient MM method to minimize the overall computational cost. The primary role of the MM layer is to constrain the geometry of the QM layer and to aid in modeling the curvature of the tube. The ωB97X-D functional, paired with the Def2SVP[33,34] basis set, was selected for the QM level calculations. The MM layer was treated using the Universal Force Field (UFF).[35] Solvent effects were accounted for using the polarized continuum model (PCM)[36,37] for water. All calculations were performed in Gaussian 16, rev. C.01.[38]

Our model of a (13,0) zigzag SWCNT with a single vacancy has 181 atoms, of which 65 are included in the QM layer, and the remaining 116 in the MM layer. Although the chemical transformations of interest are localized at the defect, the

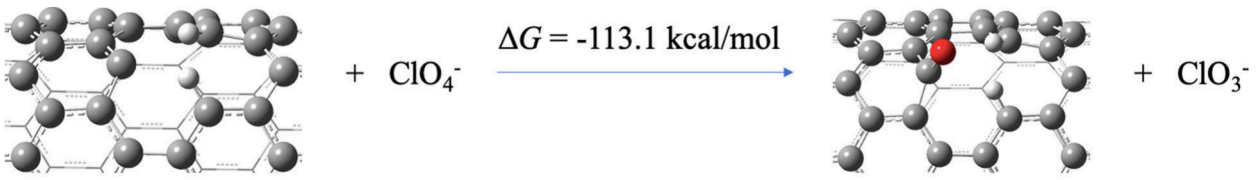

Figure 5. ClO_4^- interacting with the active carbon of the deoxy vacancy to form the ketone of the hydrolyzed form and release ClO_3^-. Oxygen is colored red, carbons gray, and hydrogens white.

https://doi.org/10.1021/acs.jpclett.4c01293
J. Phys. Chem. Lett. 2024, 15, 7788−7792

model system needs to be extended since the electronic structure of the SWCNT is a delocalized, conjugated π bonding system, and the QM/MM interface has to be sufficiently far from the active site to avoid any kind of artifact due to the segmentation of C−C bonds and H atom capping.[10] The minimal dimensions of the QM layer were carefully chosen through convergence tests to strike a balance between computational cost and accuracy. During these tests, we evaluated the energies of systems featuring nanotubes with varying numbers of carbon atoms within the QM layer, as described in Table S1. Our findings indicate that the energy discrepancy when comparing the model system reported here and a larger system can be neglected (Table S1). Smaller model systems, however, show noticeable differences, although there are instances of utilizing as few as nine carbon atoms in the QM layer.[39]

Frequency calculations were performed only on the QM portion of the nanotube to determine the free energy of the active site. Following the geometry optimization of the nanotube, using the previously described procedure, the MM portion was removed, and frequency calculations were carried out on the QM portion. The C−H bond distances were set at 1.09 Å. This approach allowed us to maintain the curvature of the active site while performing the analysis at the DFT level. We noted negligible differences in the energies obtained using the ONIOM method alone, compared to those derived from calculations focused on the active site.

We used total electronic energies of species in solution (ε_0) and added thermal corrections to the Gibbs free energy of species in vacuum (G_{corr}) to obtain their corresponding total Gibbs free energies (G_{tot}):

$$\varepsilon_0 + G_{corr} = G_{tot} \tag{1}$$

Then, we obtained the absolute potential of redox couples, E_{abs}, from $G_{tot,}$ as follows:

$$E_{abs} = -\frac{\Delta G_{tot}}{nF} \tag{2}$$

where F is the Faraday constant, n is the number of electrons involved in the redox reaction, and ΔG_{tot} is the difference between total Gibbs free energies of the two species.

ΔG_{tot} of a water molecule was obtained by using the DFT calculated electronic energy in vacuum ($\varepsilon_{0,v}$) and adding it to the empirical Gibbs free energy of solvation at −0.274 V.[40]

■ ASSOCIATED CONTENT

Supporting Information

The Supporting Information is available free of charge at https://pubs.acs.org/doi/10.1021/acs.jpclett.4c01293.

Molecular orbitals of active site structures, water hydrolysis intermediate, water, H_2O_2, and ClO_4^- interactions with the deoxy structure, vacancy regeneration process, interactions with the pristine nanotube, convergence test, active site energetics, DFT-optimized coordinates of SWCNTs and active sites are available (PDF)

■ AUTHOR INFORMATION

Corresponding Author

Victor S. Batista − *Department of Chemistry, Yale University, New Haven, Connecticut 06520, United States; Yale Energy Sciences Institute, Yale University, West Haven, Connecticut 06516, United States;* orcid.org/0000-0002-3262-1237; Email: victor.batista@yale.edu

Authors

Jana Jelušić − *Department of Chemistry, Yale University, New Haven, Connecticut 06520, United States; Yale Energy Sciences Institute, Yale University, West Haven, Connecticut 06516, United States;* orcid.org/0000-0003-1183-5954

Jan Paul Menzel − *Department of Chemistry, Yale University, New Haven, Connecticut 06520, United States; Yale Energy Sciences Institute, Yale University, West Haven, Connecticut 06516, United States;* orcid.org/0000-0002-1312-5000

Quentin C. Bertrand − *Department of Chemistry, Yale University, New Haven, Connecticut 06520, United States*

Robert H. Crabtree − *Department of Chemistry, Yale University, New Haven, Connecticut 06520, United States; Yale Energy Sciences Institute, Yale University, West Haven, Connecticut 06516, United States;* orcid.org/0000-0002-6639-8707

Hailiang Wang − *Department of Chemistry, Yale University, New Haven, Connecticut 06520, United States; Yale Energy Sciences Institute, Yale University, West Haven, Connecticut 06516, United States;* orcid.org/0000-0003-4409-2034

Gary W. Brudvig − *Department of Chemistry, Yale University, New Haven, Connecticut 06520, United States; Yale Energy Sciences Institute, Yale University, West Haven, Connecticut 06516, United States;* orcid.org/0000-0002-7040-1892

Complete contact information is available at: https://pubs.acs.org/10.1021/acs.jpclett.4c01293

Notes

The authors declare no competing financial interest.

■ ACKNOWLEDGMENTS

The authors acknowledge support by the US Department of Energy, Chemical Sciences, Geosciences, and Biosciences Division, 766 Office of Basic Energy Sciences, Office of Science (Grant DE767 FG02-07ER15909).

■ REFERENCES

(1) Prasad, V.; Vasanthkumar, M. S. Iridium-decorated multiwall carbon nanotubes and its catalytic activity with Shell 405 in hydrazine decomposition. *J. Nanopart. Res.* **2015**, *17* (10), 398.

(2) Li, Y.; Maruyama, S. *Single-Walled Carbon Nanotubes: Preparation, Properties and Applications*; Springer International Publishing: Cham, Switzerland, 2019.

(3) Patel, D. K.; Kim, H.-B.; Dutta, S. D.; Ganguly, K.; Lim, K.-T. Carbon Nanotubes-Based Nanomaterials and Their Agricultural and Biotechnological Applications. *Materials* **2020**, *13* (7), 1679.

(4) Carbon Nanotubes Market Report 2023: Single-Walled Carbon Nanotubes Lead the Charge. *Financial Services Monitor Worldwide*, 2023. https://go.exlibris.link/xcyr0NVh. (accessed 2/28/2024).

(5) Harmon, N. J.; Rooney, C. L.; Tao, Z.; Shang, B.; Raychaudhuri, N.; Choi, C.; Li, H.; Wang, H. Intrinsic Catalytic Activity of Carbon Nanotubes for Electrochemical Nitrate Reduction. *ACS Catal.* **2022**, *12* (15), 9135−9142.

(6) Fakhri, N.; Tsyboulski, D. A.; Cognet, L.; Weisman, R. B.; Pasquali, M. Diameter-dependent bending dynamics of single-walled carbon nanotubes in liquids. *Proc. Natl. Acad. Sci. U.S.A.* **2009**, *106* (34), 14219−14223.

(7) Yadav, M. D.; Joshi, H. M.; Sawant, S. V.; Dasgupta, K.; Patwardhan, A. W.; Joshi, J. B. Advances in the application of carbon nanotubes as catalyst support for hydrogenation reactions. *Chem. Eng. Sci.* **2023**, *272*, No. 118586.

(8) Nieto, J.; Jiménez, M. V.; Álvarez, P.; Pérez-Mas, A. M.; González, Z.; Pereira, R.; Sánchez-Page, B.; Pérez-Torrente, J. J.; Blasco, J.; Subias, G.; et al. Enhanced Chemical and Electrochemical Water Oxidation Catalytic Activity by Hybrid Carbon Nanotube-Based Iridium Catalysts Having Sulfonate-Functionalized NHC ligands. *ACS Appl. Energy Mater.* **2019**, *2* (5), 3283−3296.
(9) Hoque, M. A.; Gil-Sepulcre, M.; de Aguirre, A.; Elemans, J. A. A. W.; Moonshiram, D.; Matheu, R.; Shi, Y.; Benet-Buchholz, J.; Sala, X.; Malfois, M.; et al. Water oxidation electrocatalysis using ruthenium coordination oligomers adsorbed on multiwalled carbon nanotubes. *Nat. Chem.* **2020**, *12* (11), 1060−1066.
(10) Chung, L. W.; Sameera, W. M. C.; Ramozzi, R.; Page, A. J.; Hatanaka, M.; Petrova, G. P.; Harris, T. V.; Li, X.; Ke, Z.; Liu, F.; et al. The ONIOM Method and Its Applications. *Chem. Rev.* **2015**, *115* (12), 5678−5796.
(11) Tingaev, M. I.; Belenkov, E. A. Hybrid sp2+sp3 carbon phases created from carbon nanotubes. *J. Phys. Conf. Ser.* **2017**, *917* (3), No. 032013.
(12) Fang, Z.; Li, L.; Dixon, D. A.; Fushimi, R. R.; Dufek, E. J. Nature of Oxygen Adsorption on Defective Carbonaceous Materials. *J. Phys. Chem. C* **2021**, *125* (37), 20686−20696.
(13) Li, L.; Hu, J.; Shi, X.; Ruan, W.; Luo, J.; Wei, X. Theoretical Studies on Structures, Properties and Dominant Debromination Pathways for Selected Polybrominated Diphenyl Ethers. *Int. J. Mol. Sci.* **2016**, *17* (6), 927.
(14) Ma, Y.; Ma, J.; Lv, Y.; Liao, J.; Ji, Y.; Bai, H. Effect of mono vacancy defect on the charge carrier mobility of carbon nanotubes: A case study on (10, 0) tube from first-principles. *Superlattices Microstruct.* **2016**, *99*, 140−144.
(15) Su, J.; Musgrave, C. B.; Song, Y.; Huang, L.; Liu, Y.; Li, G.; Xin, Y.; Xiong, P.; Li, M. M.-J.; Wu, H.; et al. Strain enhances the activity of molecular electrocatalysts via carbon nanotube supports. *Nat. Catal.* **2023**, *6* (9), 818−828.
(16) Collins, P. G. Defects and disorder in carbon nanotubes. In *Oxford Handbook of Nanoscience and Technology: Vol. 2: Materials: Structures, Properties and Characterization Techniques*; Narlikar, A. V., Fu, Y. Y., Eds.; Oxford University Press: New York, NY, 2010; pp 31−93.
(17) Zhang, J.; Zou, H.; Qing, Q.; Yang, Y.; Li, Q.; Liu, Z.; Guo, X.; Du, Z. Effect of Chemical Oxidation on the Structure of Single-Walled Carbon Nanotubes. *J. Phys. Chem. B* **2003**, *107* (16), 3712−3718.
(18) Rossato, J.; Baierle, R. J.; Fazzio, A.; Mota, R. Vacancy Formation Process in Carbon Nanotubes: First-Principles Approach. *Nano Lett.* **2005**, *5* (1), 197−200.
(19) Kroes, J. M. H.; Pietrucci, F.; van Duin, A. C. T.; Andreoni, W. Atom Vacancies on a Carbon Nanotube: To What Extent Can We Simulate their Effects? *J. Chem. Theory Comput.* **2015**, *11* (7), 3393−3400.
(20) Kostov, M. K.; Santiso, E. E.; George, A. M.; Gubbins, K. E.; Nardelli, M. B. Dissociation of Water on Defective Carbon Substrates. *Phys. Rev. Lett.* **2005**, *95* (13), No. 136105.
(21) Ali, S.; Fu Liu, T.; Lian, Z.; Li, B.; Sheng Su, D. The effect of defects on the catalytic activity of single Au atom supported carbon nanotubes and reaction mechanism for CO oxidation. *Phys. Chem. Chem. Phys.* **2017**, *19* (33), 22344−22354.
(22) Ajayan, P. M.; Ravikumar, V.; Charlier, J. C. Surface Reconstructions and Dimensional Changes in Single-Walled Carbon Nanotubes. *Phys. Rev. Lett.* **1998**, *81* (7), 1437−1440.
(23) Singh, S.; Junaid, Z. B.; Vyas, V.; Kalyanwat, T. S.; Rana, S. S. Identification of vacancy defects in carbon nanotubes using vibration analysis and machine learning. *Carbon Trends* **2021**, *5*, No. 100091.
(24) Miao, Z.; Zhang, D.; Chen, Q. Non-enzymatic Hydrogen Peroxide Sensors Based on Multi-wall Carbon Nanotube/Pt Nanoparticle Nanohybrids. *Materials (Basel)* **2014**, *7* (4), 2945−2955.
(25) Zhang, K.; Kaufman, R. J. From endoplasmic-reticulum stress to the inflammatory response. *Nature* **2008**, *454* (7203), 455−462.
(26) Brandhuber, P.; Clark, S.; Morley, K. A review of perchlorate occurrence in public drinking water systems. *J. Am. Water Works Ass.* **2009**, *101* (11), 63−73.
(27) Greer, M. A; Goodman, G.; Pleus, R. C; Greer, S. E Health effects assessment for environmental perchlorate contamination: the dose response for inhibition of thyroidal radioiodine uptake in humans. *Environ. Health Perspect.* **2002**, *110* (9), 927−937.
(28) Ren, C.; Yang, P.; Sun, J.; Bi, E. Y.; Gao, J.; Palmer, J.; Zhu, M.; Wu, Y.; Liu, J. A Bioinspired Molybdenum Catalyst for Aqueous Perchlorate Reduction. *J. Am. Chem. Soc.* **2021**, *143* (21), 7891−7896.
(29) Frey, J. T.; Doren, D. J. *TubeGen 3.4*; University of Delaware: Newark, DE, 2011. https://turin.nss.udel.edu/research/tubegenonline.html (accessed 2/28/2023).
(30) Chai, J.-D.; Head-Gordon, M. Long-range corrected hybrid density functionals with damped atom−atom dispersion corrections. *Phys. Chem. Chem. Phys.* **2008**, *10* (44), 6615−6620.
(31) Grimme, S. Semiempirical GGA-type density functional constructed with a long-range dispersion correction. *J. Comput. Chem.* **2006**, *27* (15), 1787−1799.
(32) Svensson, M.; Humbel, S.; Froese, R. D. J.; Matsubara, T.; Sieber, S.; Morokuma, K. ONIOM: A Multilayered Integrated MO + MM Method for Geometry Optimizations and Single Point Energy Predictions. A Test for Diels−Alder Reactions and Pt(P(t-Bu)3)2 + H2 Oxidative Addition. *J. Phys. Chem.* **1996**, *100* (50), 19357−19363.
(33) Weigend, F.; Ahlrichs, R. Balanced basis sets of split valence, triple zeta valence and quadruple zeta valence quality for H to Rn: Design and assessment of accuracy. *Phys. Chem. Chem. Phys.* **2005**, *7* (18), 3297−3305.
(34) Weigend, F. Accurate Coulomb-fitting basis sets for H to Rn. *Phys. Chem. Chem. Phys.* **2006**, *8* (9), 1057−1065.
(35) Rappe, A. K.; Casewit, C. J.; Colwell, K. S.; Goddard, W. A., III; Skiff, W. M. UFF, a full periodic table force field for molecular mechanics and molecular dynamics simulations. *J. Am. Chem. Soc.* **1992**, *114* (25), 10024−10035.
(36) Improta, R.; Barone, V.; Scalmani, G.; Frisch, M. J. A state-specific polarizable continuum model time dependent density functional theory method for excited state calculations in solution. *J. Chem. Phys.* **2006**, *125* (5), No. 054103.
(37) Improta, R.; Scalmani, G.; Frisch, M. J.; Barone, V. Toward effective and reliable fluorescence energies in solution by a new state specific polarizable continuum model time dependent density functional theory approach. *J. Chem. Phys.* **2007**, *127* (7), No. 074504.
(38) Frisch, M. J.; Trucks, G. W.; Schlegel, H. B.; Scuseria, G. E.; Robb, M. A.; Cheeseman, J. R.; Scalmani, G.; Barone, V.; Petersson, G. A.; Nakatsuji, H.; Li, X.; Caricato, M.; Marenich, A. V.; Bloino, J.; Janesko, B. G.; Gomperts, R.; Mennucci, B.; Hratchian, H. P.; Ortiz, J. V.; Izmaylov, A. F.; Sonnenberg, J. L.; Williams-Young, D.; Ding, F.; Lipparini, F.; Egidi, F.; Goings, J.; Peng, B.; Petrone, A.; Henderson, T.; Ranasinghe, D.; Zakrzewski, V. G.; Gao, J.; Rega, N.; Zheng, G.; Liang, W.; Hada, M.; Ehara, M.; Toyota, K.; Fukuda, R.; Hasegawa, J.; Ishida, M.; Nakajima, T.; Honda, Y.; Kitao, O.; Nakai, H.; Vreven, T.; Throssell, K.; Montgomery, J. A., Jr.; Peralta, J. E.; Ogliaro, F.; Bearpark, M. J.; Heyd, J. J.; Brothers, E. N.; Kudin, K. N.; Staroverov, V. N.; Keith, T. A.; Kobayashi, R.; Normand, J.; Raghavachari, K.; Rendell, A. P.; Burant, J. C.; Iyengar, S. S.; Tomasi, J.; Cossi, M.; Millam, J. M.; Klene, M.; Adamo, C.; Cammi, R.; Ochterski, J. W.; Martin, R. L.; Morokuma, K.; Farkas, O.; Foresman, J. B.; Fox, D. J. *Gaussian 16 Rev. C.01*; Gaussian, Inc.: Wallingford, CT, 2016.
(39) Liu, L. V.; Tian, W. Q.; Wang, Y. A. Ozonization at the Vacancy Defect Site of the Single-Walled Carbon Nanotube. *J. Phys. Chem. B* **2006**, *110* (26), 13037−13044.
(40) Marenich, A. V.; Kelly, C. P.; Thompson, J. D.; Hawkins, G. D.; Chambers, C. C.; Giesen, D. J.; Winget, P.; Cramer, C. J.; Truhlar, D. G. *Minnesota Solvation Database − version 2012*: University of Minnesota: Minneapolis, MN, 2012. https://conservancy.umn.edu/items/c3db00cf-d573-461b-adf5-389ff929d918. (accessed 2/28/2024).

https://doi.org/10.1021/acs.jpclett.4c01293
J. Phys. Chem. Lett. 2024, 15, 7788−7792